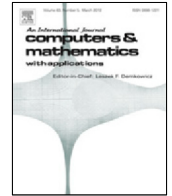




Contents lists available at ScienceDirect

Computers and Mathematics with Applications

journal homepage: www.elsevier.com/locate/camwa

Robust preconditioning for coupled Stokes–Darcy problems with the Darcy problem in primal form

Karl Erik Holter ^a, Miroslav Kuchta ^b, Kent-Andre Mardal ^{a,b,*}

^a Department of Mathematics, Division of Mechanics, University of Oslo, Oslo, Norway

^b Department of Numerical Analysis and Scientific Computing, Simula Research Laboratory, Norway

ARTICLE INFO

Article history:

Available online xxx

ABSTRACT

The coupled Darcy–Stokes problem is widely used for modeling fluid transport in physical systems consisting of a porous part and a free part. In this work we consider preconditioners for monolithic solution algorithms of the coupled Darcy–Stokes problem, where the Darcy problem is in primal form. We employ the operator preconditioning framework and utilize a fractional solver at the interface between the problems to obtain order optimal schemes that are robust with respect to the material parameters, i.e. the permeability, viscosity and Beavers–Joseph–Saffman condition. Our approach is similar to that of Holter et al. (2020), but since the Darcy problem is in primal form, expressing mass conservation at the interface involves the normal derivative, which introduces some mathematical challenges. These challenges will be specifically addressed in this paper, in particular we will employ fractional Laplacians at the interface. Numerical experiments illustrating the performance are provided. The preconditioner is posed in non-standard Sobolev spaces which may be perceived as an obstacle for its use in applications. However, we detail the implementational aspects and show that the preconditioner is quite feasible to realize in practice.

© 2020 The Authors. Published by Elsevier Ltd. This is an open access article under the CC BY license (<http://creativecommons.org/licenses/by/4.0/>).

1. Introduction

Let $\Omega = \Omega_f \cup \Omega_p$, where Ω_f is the domain of the viscous flow, Ω_p is the domain of the porous media and Γ their common interface. Further let the domain boundaries be decomposed as $\partial\Omega_f = \Gamma \cup \partial\Omega_{f,D} \cup \partial\Omega_{f,N}$ and $\partial\Omega_p = \Gamma \cup \partial\Omega_{p,D} \cup \partial\Omega_{p,N}$, where subscripts D, N signify respectively that Dirichlet and Neumann boundary conditions are prescribed on the part of the boundary. The boundary of Γ , i.e., the intersection of Γ and $\partial\Omega$ is denoted by $\partial\Gamma$. An illustration is given in Fig. 1.

The Stokes problem reads:

$$\mu \Delta \mathbf{u}_f - \nabla p_f = \mathbf{f} \text{ in } \Omega_f, \quad (1)$$

$$\nabla \cdot \mathbf{u}_f = 0 \text{ in } \Omega_f, \quad (2)$$

while the Darcy problem in primal form reads:

$$-K \Delta p_p = g \text{ in } \Omega_p. \quad (3)$$

* Corresponding author at: Department of Mathematics, Division of Mechanics, University of Oslo, Oslo, Norway.

E-mail addresses: karleh@math.uio.no (K.E. Holter), miroslav@simula.no (M. Kuchta), kent@math.uio.no (K.-A. Mardal).

<https://doi.org/10.1016/j.camwa.2020.08.021>

0898-1221/© 2020 The Authors. Published by Elsevier Ltd. This is an open access article under the CC BY license (<http://creativecommons.org/licenses/by/4.0/>).

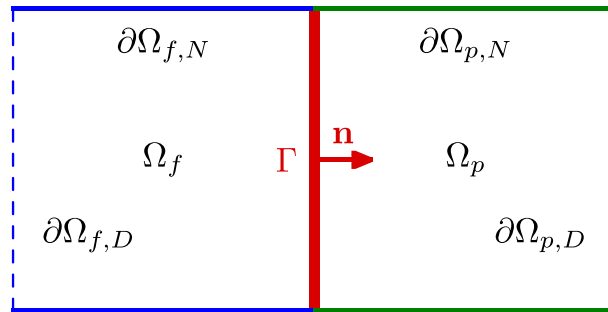


Fig. 1. Schematic domain of Darcy–Stokes problem. Dirichlet conditions shown in dashed line, and interface in red. (For interpretation of the references to color in this figure legend, the reader is referred to the web version of this article.)

Here, \mathbf{u}_f, p_f are the unknown velocity and pressure for the Stokes problem (1)–(2) in Ω_f , p_p is the unknown pressure of the Darcy problem (3) in Ω_p . The material parameters are the fluid viscosity μ and the permeability K . Here we shall consider the problem with the Dirichlet boundary conditions

$$\mathbf{u}_f = \mathbf{u}_f^0 \text{ on } \partial\Omega_{f,D}, \quad p_p = p_p^0 \text{ on } \partial\Omega_{p,D}$$

and Neumann conditions

$$(\mu \nabla \mathbf{u}_f - p_f \mathbf{I}) \cdot \mathbf{n}_f = \mathbf{h} \text{ on } \partial\Omega_{f,N}, \quad \nabla p_p \cdot \mathbf{n}_p = h_p \text{ on } \partial\Omega_{p,N},$$

where $\mathbf{n}_f, \mathbf{n}_p$ are the outer unit normals of the respective subdomains. In particular we assume that $|\partial\Omega_{i,D}| > 0$ and $|\partial\Omega_{i,N}| > 0$ for $i = p, f$. Moreover, the coupled problem must be equipped with interface conditions expressing the continuity of stress as well as mass balance. We postpone their description until we describe the weak formulation of the problem.

The discretization of the coupled Darcy–Stokes problem with the Darcy problem in a mixed form is challenging since the Darcy and Stokes problems, respectively, call for different schemes. For example, typical finite element methods for the Darcy problem, like the Raviart–Thomas or Brezzi–Douglas–Marini elements, are not stable for Stokes problem as the discretization of the flux specifically targets the properties of $H(\text{div})$ rather than H^1 which is natural for Stokes discretizations. For this reason, a wide range of methods have been proposed over the last decade that address this particular challenge. For example, new elements robust for both the Darcy and Stokes problem have been proposed in [1–5]. Alternatively, stabilization or modifications of standard methods may be used as in [6–10]. In this work we will consider the coupled problem with the Darcy equation in a primal form and a Lagrange multiplier to couple the Stokes and Darcy problems. Standard elements in both the Darcy and the Stokes domain can then be used, but a main problem with such schemes is the stability of the discretization at the interface.

The well-posedness of the Darcy–Stokes problem coupled together through the use of a Lagrange multiplier is well-known when the Darcy problem is in mixed form [11,12], where both the continuous setting and various discretizations were proposed. Other solution and discretization algorithms for the coupled problem are presented in e.g. [13,14], see [11,15] for an overview. For the mixed formulation we have, in our previous work [16], developed monolithic solvers that are robust with respect to all material parameters by utilizing fractional solvers on the interface. Here, we continue with the same type of approach, but address the difficulty of the Darcy problem in primal form, where the main concern from a mathematical point of view is the normal gradient at the interface. However, as the interface is of lower dimension, the number of degrees of freedom at the interface is typically small compared to the overall problem and preconditioning blocks at the interface based on fractional Laplacians are hence feasible to realize without sacrificing performance. Furthermore, multilevel solvers are available for fractional Laplacians [17,18] if the interface requires more degrees of freedom than can be solved for by direct methods. We remark that the problem to be studied further is symmetric and includes an explicit variable, the Lagrange multiplier, on Γ . In this respect it differs from the more common primal formulation, which leads to a non-symmetric system to be solved for \mathbf{u}_f, p_f and p_p . Well-posedness of the latter problem was established in [15] with efficient solvers proposed and analyzed e.g. in [19–21].

An outline of the paper is as follows: Section 2 describes the notation, introduces the symmetric primal Darcy–Stokes problem and illustrates the difficulties in its preconditioning. The main challenge for the solver construction, i.e. the proper posing of the coupling operator, is addressed in Section 3. Parameter robust preconditioners are then established in Section 4.

2. Preliminaries

Let Ω be a bounded Lipschitz domain in \mathbb{R}^n , $n = 2$ or 3 , and denote its boundary by $\partial\Omega$. We denote by $L^2(\Omega)$ the Lebesgue space of square integrable functions, with the norm $\|u\|_{L^2(\Omega)}^2 = \int_{\Omega} |u|^2 dx$, and by $H^1(\Omega)$ the Sobolev space of

functions with first derivative in $L^2(\Omega)$ with norm $\|u\|_{H^1(\Omega)}^2 = \|u\|_{L^2(\Omega)}^2 + \|\nabla u\|_{L^2(\Omega)}^2$. Note that the spaces are both Hilbert spaces, with the standard inner products. These spaces are defined in the same way when u is a vector field, in which case we will write \mathbf{u} in boldface. We also define the subspace $H_0^1(\Omega)$ to be the completion in $\|\cdot\|_{H^1(\Omega)}$ of $C_0^\infty(\Omega)$, the space of smooth functions on Ω whose restriction to $\partial\Omega$ is zero.

For a Lipschitz domain Ω with $\Gamma \subset \partial\Omega$, we can define a trace operator T by $Tu = u|_\Gamma$ for smooth u . This can be extended to a bounded, surjective and right-invertible operator $H^1(\Omega) \rightarrow H^{\frac{1}{2}}(\Gamma)$ (cf. e.g. [22]), where the space $H^{\frac{1}{2}}(\Gamma)$ will be defined later. Given a subset $\partial\Omega_D$ of $\partial\Omega$, we let $H_{0,\partial\Omega_D}^1(\Omega)$, or for readability just $H_{0,D}^1(\Omega)$, be the subspace of $H^1(\Omega)$ for which the restriction to $\partial\Omega_D$ is zero, where the restriction is defined in terms of the trace operator. Typically, $\partial\Omega_D$ will be the subset of $\partial\Omega$ on which Dirichlet conditions are prescribed. We also define the semi-norm $L_\tau^2(\Gamma)$ on $H^1(\Omega)$ to be the $L^2(\Gamma)$ norm of the tangential component of \mathbf{u} at Γ . In 2D, this is just $\|\mathbf{u}|_\Gamma \cdot \boldsymbol{\tau}\|_{L^2(\Gamma)}$ where $\boldsymbol{\tau}$ is a tangent unit vector, while in 3D it is more conveniently written as $\|\mathbf{u}|_\Gamma - (\mathbf{u}|_\Gamma \cdot \mathbf{n})\mathbf{n}\|_{L^2(\Gamma)}$.

For any inner product space X , we let $(\cdot, \cdot)_X$ denote its inner product. When $X = L^2(\Omega)$, we will omit the subscript if there is no cause for confusion. We write the space of continuous linear operators from X to Y as $\mathcal{L}(X, Y)$, or just as $\mathcal{L}(X)$ if $Y = X$. For any two Sobolev spaces X, Y both contained in a common ambient space, we define the intersection and sum spaces $X \cap Y$ and $X + Y$ in terms of the norms

$$\|u\|_{X \cap Y}^2 = \|u\|_X^2 + \|u\|_Y^2 \quad \text{and} \quad \|u\|_{X+Y}^2 = \inf_{x+y=u} \|x\|_X^2 + \|y\|_Y^2.$$

For any $c > 0$, we define the scaled space cX to be just X as a set, but with the inner product $(u, v)_{cX} = c(u, v)_X$. Its norm is trivially equivalent to $\|\cdot\|_X$, but because the equivalence constant depends on c , the distinction between the two norms becomes important when we need to establish the independence of bounds with respect to problem parameters.

We define the fractional space $H^s(\Gamma)$ following [23]. Let $S \in \mathcal{L}(H^1(\Gamma))$ be the operator such that $(Su, v)_{H^1} = (S(I - \Delta)u, v) = (u, v)_{L^2}$ for all $v \in H^1(\Gamma)$. We can then find a basis of $H^1(\Gamma)$ of orthonormal eigenfunctions e_i of S with eigenvalues $\lambda_i > 0$. Writing $u = \sum_i c_i e_i$ in this basis, we define the norm $\|u\|_{H^s(\Gamma)}^2 = \sum c_i^2 \lambda_i^{-s}$ for any $s \in [-1, 1]$. Further, let the space $H^s(\Gamma)$ be the completion of $C^\infty(\Gamma)$ with respect to $\|\cdot\|_{H^s(\Gamma)}$. We also define the space $H_{00}^s(\Gamma)$ in the same manner, except that we then apply Dirichlet boundary conditions by choosing S in $\mathcal{L}(H_0^1(\Gamma))$. Furthermore, $H_{00}^s(\Gamma)$ is the completion of $C_0^\infty(\Gamma)$ rather than $C^\infty(\Gamma)$.

For the sake of completeness we review here the construction of a matrix realization of fractional operators given in [23]. To this end let $V_h \subset H^1(\Gamma)$, $n = \dim V_h$, be a finite dimensional finite element subspace with basis functions ϕ_i , $i = 1, \dots, n$ and $\mathbf{A}, \mathbf{M} \in \mathbb{R}^{n \times n}$ be the symmetric positive definite (stiffness and mass) matrices such that

$$\mathbf{A}_{ij} = (\nabla \phi_j, \nabla \phi_i) \quad \text{and} \quad \mathbf{M}_{ij} = (\phi_j, \phi_i).$$

In case $V_h \not\subset H^1(\Gamma)$ and piecewise constant (P0) discretization is used we let

$$\mathbf{A}_{ij} = \sum_{v \in \mathcal{N}} \{ \{h\} \}_v^{-1} (\llbracket \phi_j \rrbracket_v, \llbracket \phi_i \rrbracket_v)_v,$$

where \mathcal{N} is a set of all the facets of the finite element mesh. Further the (facet) average and jump operators are defined as $\{ \{u\} \}_v = \frac{1}{2}(u|_{K^+} + u|_{K^-})$, $\llbracket u \rrbracket_v = u|_{K^+} - u|_{K^-}$ with K^+ and K^- the two cells sharing facet v . When v is an exterior facet, we define $\llbracket u \rrbracket_v = \{ \{u\} \}_v = u|_K$, where K is the unique cell with v as facet.

It follows that the generalized eigenvalue problem $(\mathbf{A} + \mathbf{M})\mathbf{u} = \mathbf{M}\mathbf{u}\lambda$ has only positive eigenvalues and a complete set of eigenvectors that form the basis of \mathbb{R}^n so that the powers of $\mathbf{S} = \mathbf{U}\boldsymbol{\Lambda}(\mathbf{M}\mathbf{U})^T$ are well defined. For $s \in [-1, 1]$ we then set $\mathbf{H}(s) = \mathbf{M}\mathbf{S}^s$. Letting \mathbf{u} be the vector of degrees of freedom of $u_h \in V_h$, i.e. $u_h = \sum_i^n u_i \phi_i$, we finally have

$$\|u_h\|_{H^s} = \sqrt{\sum_{i,j=1}^n u_i \mathbf{H}_{ij}(s) u_j}.$$

When \mathbf{u} is a vector function, we define the normal trace $T_n \mathbf{u} = \mathbf{u}|_\Gamma \cdot \mathbf{n}$ using the trace operator T component-wise. As such T_n is a continuous map $H^1(\Omega) \rightarrow H^{\frac{1}{2}}(\Gamma)$. Moreover, we let T_τ be the tangential trace operator. We remark that in 2D and 3D the operator maps to scalar, respectively vector fields. The normal derivative, $\partial_n u = \nabla u \cdot \mathbf{n}|_\Gamma$, is more challenging to define properly in this context. Let us therefore briefly sketch an approach, which at least in the authors' opinion at first glance seems like a natural starting point. However, as we will show, the approach does not yield robust preconditioners in our context. First, notice that if we impose additional regularity on u and require that $\Delta u \in L^2$ then ∂_n is well defined. In detail, let $w \in H^{1/2}(\partial\Omega)$ and $E : H^{1/2}(\partial\Omega) \rightarrow H^1(\Omega)$ be a (harmonic) extension operator. Then $\partial_n u$ clearly lies in $H^{-1/2}(\partial\Omega)$ because

$$\int_{\partial\Omega} \partial_n u \cdot \mathbf{w} \, ds = \int_{\Omega} \Delta u \cdot E\mathbf{w} \, dx + \int_{\Omega} \nabla \cdot (E\mathbf{w}) \cdot \nabla u \, dx \leq \infty.$$

This extra regularity assumption is, however, hard to express in the operator preconditioning framework. In particular, to the authors' knowledge, there are no *standard* finite elements that would enable us to exploit the extra regularity. A

possible approach could be NURBS [24] or C^1 discretizations developed for fourth order problems. However, the latter often show poor performance for second order problems [25].

Alternatively, we may attempt to define ∂_n as a composition of the first order derivative operator, ∇ , with the 1/2 order normal trace operator T_n . The composition ∂_n could then be expected to be a 3/2 operator $\partial_n : H^1(\Omega) \rightarrow H^{-1/2}(\partial\Omega)$. From an operator preconditioning point of view, this would be feasible to realize, as we will see below. However, as we will demonstrate, robustness will not be obtained if we realize ∂_n as a 3/2 operator. In fact, robustness is only obtained if ∂_n is a first order operator, $\partial_n : H^1(\Omega) \rightarrow L^2(\partial\Omega)$. We remark here that while the operator in a continuous setting is $\partial_n : H^1(\Omega) \rightarrow L^2(\partial\Omega)$, in the discrete setting we will include a scaling parameter, i.e. the mesh size, because we use the finite element method. To see that this is reasonable, notice that for finite elements, the mass matrix, as representation of the identity, is differently scaled in different dimensions. In Example 3.2 we detail the scaling in a simplified example.

In order to demonstrate why posing the ∂_n operator properly is required, let us now formulate the coupled Darcy–Stokes problem, where the Darcy problem is in a primal form. As a starting point, let the Lagrangian of the coupled problem be,

$$L(\mathbf{u}_f, p_f, p_p, \lambda) = \int_{\Omega_f} \frac{1}{2} (\mu(\nabla \mathbf{u}_f)^2 - \mathbf{f} \cdot \mathbf{u}_f) \, dx + \int_{\Gamma} \frac{1}{2} D(\mathbf{u}_f \cdot \boldsymbol{\tau})^2 \, ds + \int_{\Omega_p} \frac{1}{2} K ((\nabla p_p)^2 - g p_p) \, dx + \int_{\Omega_f} \nabla \cdot \mathbf{u}_f p_f \, dx + \int_{\Gamma} (T_n \mathbf{u}_f - K \partial_n p_p) \lambda \, ds.$$

Note that the sign of p_f has been changed from (1). Here, the Lagrange multiplier λ in $\int_{\Gamma} (T_n \mathbf{u}_f - K \partial_n p_p) \lambda \, ds$ is used to ensure mass conservation, while the extra term $\int_{\Gamma} \frac{1}{2} D(\mathbf{u}_f \cdot \boldsymbol{\tau})^2 \, ds$, where $D = \alpha_{\text{BJS}} \sqrt{\frac{\mu}{k}}$ corresponds to the Beavers–Joseph–Saffman condition [26].

The corresponding weak formulation is obtained by the first order optimality conditions of the Lagrangian, that is; $\frac{\partial L}{\partial \mathbf{u}_f} = 0$, $\frac{\partial L}{\partial p_f} = 0$, $\frac{\partial L}{\partial p_p} = 0$, and $\frac{\partial L}{\partial \lambda} = 0$. A variational formulation hence reads: Find $(\mathbf{u}_f, p_p, p_f, \lambda)$ such that

$$a((\mathbf{u}_f, p_p), (\mathbf{v}_f, q_p)) + b((\mathbf{v}_f, q_p), (p_f, \lambda)) = f((\mathbf{v}_f, q_p)) \quad \forall (\mathbf{v}_f, q_p), \\ b((\mathbf{u}_f, p_p), (q_f, w)) = g((q_f, w)) \quad \forall (q_f, w), \tag{4}$$

where the bilinear forms a, b are defined as

$$a((\mathbf{u}_f, p_p), (\mathbf{v}_f, q_p)) = \mu(\nabla \mathbf{u}_f, \nabla \mathbf{v}_f)_{\Omega_f} + D(\mathbf{u}_f \cdot \boldsymbol{\tau}, \mathbf{v}_f \cdot \boldsymbol{\tau})_{\Gamma} + K(\nabla p_p, \nabla q_p)_{\Omega_p}, \\ b((\mathbf{u}_f, p_p), (q_f, w)) = (\nabla \cdot \mathbf{u}_f, q_f)_{\Omega_f} + (T_n \mathbf{u}_f, w)_{\Gamma} - K(\partial_n p_p, w)_{\Gamma}. \tag{5}$$

We shall refer to (4) as the (primal) Darcy–Stokes problem. Note that the resulting formulation is symmetric.

While appropriate function spaces are readily available for \mathbf{u}_f, p_p, p_f and their corresponding test functions, it is less clear what the appropriate requirements are for w and λ . This will be addressed below.

Example 2.1 (Preconditioner for coupled Darcy–Stokes problem assuming $\partial_n : H^1 \rightarrow H^{-1/2}$). Let us assume that ∂_n is a 3/2 operator so that $K \partial_n p_p \in \frac{1}{\sqrt{k}} H^{-1/2}$ for $p_p \in \sqrt{k} H_{0,D}^1(\Omega_p)$. Next, observe that since $\mathbf{u}_f \in \sqrt{\mu} H_{0,D}^1(\Omega_f) \cap \sqrt{D} L_{\tau}^2(\Gamma)$ then $T_n \mathbf{u}_f \in \sqrt{\mu} H^{1/2}$. Per assumption the coupling term $T_n \mathbf{u}_f - K \partial_n p_p$ belongs to $\sqrt{\mu} H^{1/2} + \frac{1}{\sqrt{k}} H^{-1/2}$ so that the dual variable $w \in \frac{1}{\sqrt{\mu}} H^{-1/2} \cap \sqrt{k} H^{1/2}$. In turn, we consider the following weak formulation: Find $\mathbf{u}_f, p_p, p_f, \lambda \in \sqrt{\mu} H_{0,D}^1(\Omega_f) \cap \sqrt{D} L_{\tau}^2(\Gamma), \sqrt{k} H_{0,D}^1(\Omega_p), \frac{1}{\sqrt{\mu}} L^2(\Omega_f), \frac{1}{\sqrt{\mu}} H^{-1/2} \cap \sqrt{k} H^{1/2}$ such that

$$a((\mathbf{u}_f, p_p), (\mathbf{v}_f, q_p)) + b((\mathbf{v}_f, q_p), (p_f, \lambda)) = f((\mathbf{v}_f, q_p)) \quad \forall (\mathbf{v}_f, q_p) \in \sqrt{\mu} H_{0,D}^1(\Omega_f) \cap \sqrt{D} L_{\tau}^2(\Gamma) \times \frac{1}{\sqrt{\mu}} L^2(\Omega_f), \\ b((\mathbf{u}_f, p_p), (q_f, w)) = g((q_f, w)) \quad \forall (q_f, w) \in \sqrt{k} H_{0,D}^1(\Omega_p) \times \frac{1}{\sqrt{\mu}} H^{-1/2} \cap \sqrt{k} H^{1/2}. \tag{6}$$

The coefficient matrix associated with (4) reads

$$\mathcal{A} = \left(\begin{array}{cc|cc} -\mu \Delta + D T_{\tau}' T_{\tau} & & (\nabla \cdot)' & T_n' \\ & -K \Delta & & -K \partial_n' \\ \hline & \nabla \cdot & & \\ & T_n & & -K \partial_n \end{array} \right). \tag{7}$$

Assuming that the proposed spaces indeed lead to a well-posed operator \mathcal{A} , the operator preconditioning framework [27] yields as a preconditioner the Riesz mapping

$$\mathcal{B} = \left(\begin{array}{cc|cc} -\mu \Delta + D T_{\tau}' T_{\tau} & & & \\ & -K \Delta & & \\ \hline & & \frac{1}{\mu} I & \\ & & & \frac{1}{\mu} (I + \Delta)^{-1/2} + K (I + \Delta)^{1/2} \end{array} \right)^{-1}. \tag{8}$$

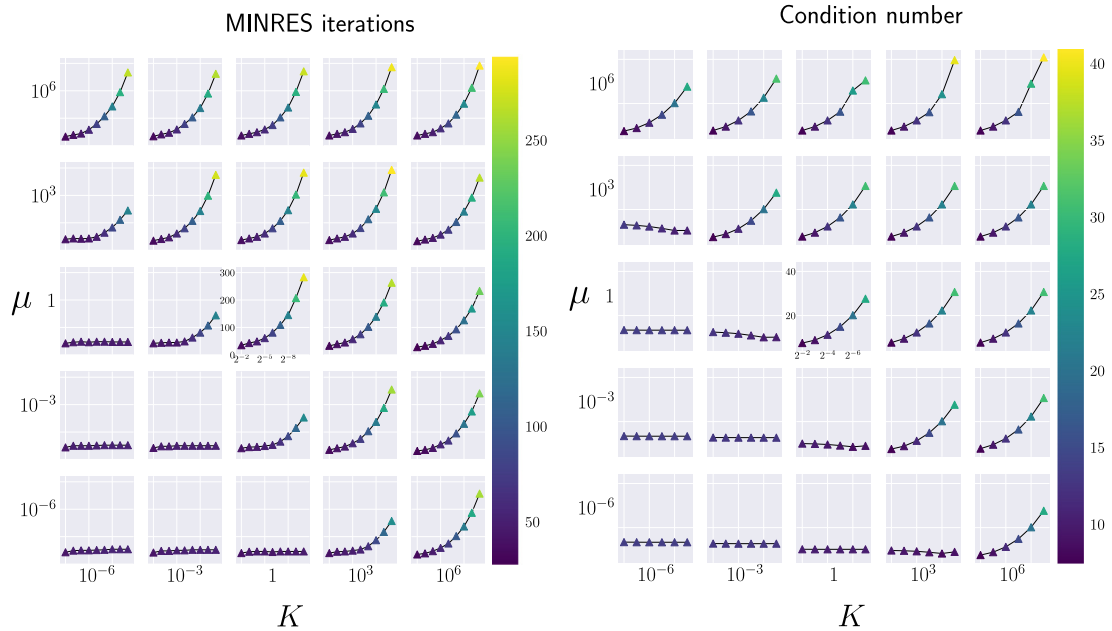


Fig. 2. Mesh refinement vs. iteration counts (left) and condition numbers (right) for Example 2.1. All subplots share x- and y-axes. For fixed μ , K the x-axis range in the iterations subplot extends from (mesh size) $h = 2^{-2}$ to $h = 2^{-10}$. In the condition number plots the range is from $h = 2^{-2}$ to $h = 2^{-8}$. In all cases, $\alpha_{BFS} = 1$.

In order to test the preconditioner, we solve problem (6) on $\Omega = [0, 2] \times [0, 1]$, where $\Omega_f = [0, 1] \times [0, 1]$ and $\Omega_p = [1, 2] \times [0, 1]$ and the Dirichlet boundary domains are $\partial\Omega_{f,D} = \{(x, y) \in \partial\Omega_f, x = 0\}$ and $\partial\Omega_{p,D} = \{(x, y) \in \partial\Omega_p, x = 2\}$, cf. Fig. 1. The mesh is a uniform triangular mesh, consisting of $4N^2$ equally sized isosceles triangles. To discretize (4), we use lowest order (P2-P1) Taylor–Hood elements for the Stokes velocity and pressure, while piecewise quadratic elements (P2) were used for the Darcy pressure and piecewise constant elements (P0) for the Lagrange multiplier. Discretization is carried out in the FEniCS library [28], with coupling maps between the interface and domains and the fractional Laplacians being implemented by the extension FEniCS_{ii} [29].

Approximation of the preconditioner (8) is constructed by using single sweep of V-cycle of algebraic multigrid BoomerAMG from the Hypr library [30] for all the blocks except for the interface block, which is inverted exactly. Starting from a random initial vector, we count the number of iterations required to solve the preconditioned linear system using the MINRES solver from the PETSc library [31] with convergence criterion based on relative tolerance of 10^{-8} and absolute tolerance of 10^{-10} . Additionally, the condition numbers of $\mathcal{B}^{-1}\mathcal{A}$ are computed using an iterative solver from the SLEPc library [32]. In the condition number computations the operator \mathcal{B} is computed exactly, that is, all the blocks are inverted by LU. We remark that this solver setup is used also in the subsequent examples.

The results of the experiment are plotted in Fig. 2. By the failure of the iteration counts to stabilize, we see that using $\frac{1}{\mu}(I + \Delta)^{-1/2} + K(I + \Delta)^{1/2}$ as multiplier space does not lead to a robust preconditioner over the whole parameter range. Note, however, that in the regime where μ is significantly smaller than K (i.e. the lower left region of the plots in Fig. 2), iteration counts and condition numbers appear to be stable as the mesh is refined. In this regime, the norm of the multiplier space is dominated by the part from $\frac{1}{\sqrt{\mu}}H^{-1/2}$, which is determined by posing of the trace operator. This suggests that the choice of $\sqrt{KH}^{1/2}$, i.e. wrong posing of the ∂_n operator, is responsible for the lack of boundedness.

3. Approximating the trace normal gradient operator

A crucial step in the analysis of the Darcy–Stokes problem will be the mapping properties of the operator ∂_n . As a computationally practical choice of space for the Darcy pressure is \sqrt{KH}^1 , we immediately run into the problem discussed in the preliminaries because ∂_n cannot be defined on all of H^1 . This necessitates either an assumption of extra regularity or an alternative approach.

Motivated by the observation in [33], that in a discrete finite element setting the trace operator is stable as a map $L^2(\Omega) \rightarrow L^2(\partial\Omega)$, we propose an alternative approach to construct the preconditioners. We start off by outlining the construction of an operator $\partial_{n,\epsilon} : H^1(\Omega_p) \rightarrow L^2(\Gamma)$ which will be an approximation to ∂_n . Suppose Γ is a sufficiently regular subset of $\partial\Omega_p$, and that Γ is of co-dimension 1 in Ω_p . The ϵ -thick envelope $\Gamma_\epsilon = \{y \in \Omega_p, \text{dist}(y, \Gamma) < \epsilon\}$ is a

higher-dimensional approximation of Γ . For any $v \in H^1(\Omega_p)$,

$$\frac{1}{\epsilon} \int_{\Gamma_\epsilon} v \phi \, dx \rightarrow \int_{\Gamma} T v T \phi \, ds \text{ as } \epsilon \rightarrow 0, \tag{9}$$

where ϕ is a test function in $H^1(\Omega_p)$.

Note that although the integral over Γ is not well-defined for a general $v \in L^2(\Omega_p)$, the integral over Γ_ϵ is. Provided Γ is sufficiently regular and ϵ sufficiently small, we assume that there exists a vector field $\mathbf{n}_{\Gamma_\epsilon}$ on Γ_ϵ which approximates the normal vector \mathbf{n}_Γ of Γ at Γ . Using $\mathbf{n}_{\Gamma_\epsilon}$, we further assume that we can define a bounded extension $E_\epsilon : L^2(\Gamma) \rightarrow L^2(\Gamma_\epsilon)$ along $\mathbf{n}_{\Gamma_\epsilon}$ for which $\int_{\Gamma_\epsilon} w \, ds \approx \frac{1}{\epsilon} \int_{\Gamma_\epsilon} E_\epsilon w \, dx$ for any $w \in L^2(\Gamma)$. Provided $\mathbf{n}_{\Gamma_\epsilon}$ and E_ϵ can be defined, then for any $u \in H^1(\Omega_p)$ we can define $\partial_{\mathbf{n},\epsilon} u$ by

$$\int_{\Gamma} \partial_{\mathbf{n},\epsilon} u \cdot w \, ds = \frac{1}{\epsilon} \int_{\Gamma_\epsilon} \nabla u \cdot \mathbf{n}_{\Gamma_\epsilon} E_\epsilon w \, dx$$

for any $w \in L^2(\Gamma)$, thus defining the required map $\partial_{\mathbf{n},\epsilon} : H^1(\Omega_p) \rightarrow L^2(\Gamma_\epsilon)$ approximating $\partial_{\mathbf{n}}$. We assume that the resulting operator $\partial_{\mathbf{n},\epsilon}$ is both surjective and bounded, with $\|\partial_{\mathbf{n},\epsilon} u\|_{L^2(\Gamma_\epsilon)} \leq C \|u\|_{H^1(\Omega_p)}$, and that $\partial_{\mathbf{n},\epsilon}$ has a bounded right inverse.

We emphasize that $\partial_{\mathbf{n},\epsilon}$ is just an analytical tool constructed for the analysis in the continuous setting and that ϵ is not related to the mesh size h . In fact, we can choose ϵ far smaller than the mesh size and for any practical purposes in computations we assume that $\partial_{\mathbf{n},\epsilon}$ will be practically identical to $\partial_{\mathbf{n}}$. We summarize the assumption as follows:

Assumption 1. Given a sufficiently regular $\Gamma \subset \partial\Omega_p$, $\partial_{\mathbf{n},\epsilon} : H^1(\Omega_p) \rightarrow L^2(\Gamma_\epsilon)$ is a bounded surjection which approximates $\partial_{\mathbf{n}}$ on the subspace of H^1 on which $\partial_{\mathbf{n}}$ can be defined. Further, $\partial_{\mathbf{n},\epsilon}$ has a bounded right inverse.

Although characterizing the conditions under which **Assumption 1** holds is beyond the scope of this paper, we motivate the existence of the required constructions $E_\epsilon, \mathbf{n}_\epsilon$ in a few simple examples below.

Example 3.1. Let Γ be the y -axis, and Ω_p be the positive half-plane. The construction of $E_\epsilon, \mathbf{n}_{\Gamma_\epsilon}$ is then given by $\mathbf{n}_{\Gamma_\epsilon} = \mathbf{n}_\Gamma = (-1, 0)$ and for $w(y) \in C^1(\Gamma)$ we let $(E_\epsilon w)(x, y) = w(y)$. This continuously extends to all of $L^2(\Gamma)$. Clearly $\partial_{\mathbf{n},\epsilon} u \rightarrow \partial_{\mathbf{n}} u$ as $\epsilon \rightarrow 0$ for $u \in C^1$. Given any $w(y) \in C^0(\Gamma)$, define u by $u(x, y) = -xw(y)$. Then the map $w \rightarrow u$ continuously extends to a right inverse of $\partial_{\mathbf{n},\epsilon}$, as by linearity $\partial_{\mathbf{n},\epsilon} u = \partial_{\mathbf{n}} u = w$.

Next, suppose Ω_p is the unit disk, and Γ its boundary. By parametrizing Γ with e.g. polar coordinates, this case can be effectively translated to the above. $\mathbf{n}_{\Gamma_\epsilon}$ is now the unit radial vector \mathbf{i}_r , and for any $w(\theta) \in C^1(\Gamma)$, $(E_\epsilon w)(r, \theta) = w(\theta)$. Again, this definition of E_ϵ extends to all of $L^2(\Gamma)$. Because $\frac{1}{\epsilon} \int_{\Gamma_\epsilon} \nabla u \cdot \mathbf{n}_{\Gamma_\epsilon} E_\epsilon w \, dx = \int_0^{2\pi} w(\theta) \cdot \int_{1-\epsilon}^1 \frac{1}{\epsilon} \frac{\partial u}{\partial r} r \, dr \, d\theta$ and $\frac{1}{\epsilon} \int_{1-\epsilon}^1 f(r) \, dr \rightarrow f(1)$ as $\epsilon \rightarrow 0$, we again have $\partial_{\mathbf{n},\epsilon} u \rightarrow \partial_{\mathbf{n}} u$ as $\epsilon \rightarrow 0$ for $u \in C^1$. Analogously to the previous case, a right inverse can be defined by sending any $w(\theta) \in C^0(\Gamma)$ to $u(r, \theta) = rw(\theta)$.

Before considering the Darcy–Stokes problem, we justify **Assumption 1**. First we consider a simplified example in order to illustrate how the scaling of mass matrices in different dimensions affects preconditioners constructed via the application of trace operators. Then, in **Example 3.3** we construct preconditioners for a Poisson problem with a $\partial_{\mathbf{n}}$ -constraint which is to be enforced by a Lagrange multiplier, cf. the Babuška problem [34] involving the trace operator.

Example 3.2 (Trace Constrained L^2 Projection). Let Ω be a bounded domain with $\Gamma \subseteq \partial\Omega$ and $V = H^1(\Omega)$. We then consider the problem

$$\min_{u \in V} \int_{\Omega} u^2 \, dx - 2 \int_{\Omega} f u \, dx \quad \text{subject to} \quad \int_{\Gamma} (Tu - g) p \, ds = 0. \tag{10}$$

Letting p denote the Lagrange multiplier associated with the boundary constraint, the extrema $u \in V, p \in Q = L^2(\Gamma)$ of the Lagrangian of (10) satisfy the variational problem: Find $u \in V$ and $p \in Q$ such that

$$\begin{aligned} \int_{\Omega} uv \, dx + \int_{\Gamma} p T v \, ds &= \int_{\Omega} f v \, dx \quad \forall v \in V, \\ \int_{\Gamma} q T u \, ds &= \int_{\Gamma} g q \, ds \quad \forall q \in Q. \end{aligned} \tag{11}$$

The operator of the preconditioned continuous problem then reads

$$\mathcal{BA} = \begin{pmatrix} I & \\ & S \end{pmatrix}^{-1} \begin{pmatrix} I & T' \\ & T \end{pmatrix}, \tag{12}$$

where S is to be constructed such that the condition number of the discrete problems is bounded in the discretization parameter h . Here we shall consider three constructions. We remark that when using the finite element realization of the identity operator, we mean the mass matrix and denoted it by I . The mass matrix has eigenvalues such that both the smallest and largest eigenvalues scale as h^d on uniform mesh. First we consider $S = I$, with eigenvalues $\approx h$ because

Table 3.1

Condition numbers of (12) with different preconditioners and discretization by P2-P1 elements on (us) mesh from Fig. 3. Boundedness is obtained with the Schur complement preconditioner $h^{-1}I$.

h	I	$(-\Delta + I)^{-1/2}$	$h^{-1}I$
2^{-2}	8.72	24.08	4.63
2^{-3}	12.11	47.84	4.63
2^{-4}	16.91	95.15	4.63
2^{-5}	23.70	189.9	4.63
2^{-6}	33.31	379.2	4.63
2^{-7}	46.90	758.0	4.63
2^{-8}	66.12	1515	4.63

Table 3.2

Condition numbers of (12) with preconditioner using $S = h^{-1}I$. Boundedness with different types of triangulations, cf. Fig. 3, and discretizations can be observed.

l	P2-P1			P2-P0		
	(us)	(uu)	(nu)	(us)	(uu)	(nu)
1	4.63	4.63	4.10	4.63	4.63	3.98
2	4.63	4.06	4.32	4.63	4.07	4.33
3	4.63	4.20	4.28	4.63	4.20	4.31
4	4.63	4.29	4.31	4.63	4.32	4.34
5	4.63	4.45	4.50	4.63	4.43	4.45
6	4.63	4.25	4.28	4.63	4.32	4.37
7	4.63	4.25	4.36	4.63	4.28	4.39

Γ is a 1D manifold. Then, following [33], we let $S = h^{-1}I$, i.e., a matrix with eigenvalues ≈ 1 . Finally, the choice of $S = (-\Delta + I)^{-1/2}$ is included to show that the relevant trace space in (12) is not (by viewing the trace as an order 1/2 operator) $H^{1/2}$ so that dual variable would reside in $H^{-1/2}$.

We remark that the first two operators are in practical computations assembled as weighted mass matrices where the weights for the respective operators are 1 and inverse cell volume. Recalling Section 2 the matrix representation of the fractional operator is $H(1/2)$.

To compare the three preconditioners, we let Ω be a unit square, $\Gamma = \{(x, y) \in \partial\Omega, x = 0\}$. Further, the domain shall be discretized uniformly into $4N^2$ isosceles triangles with size $h = 1/N$, see Fig. 3. Such discretization shall be in the following referred to as uniformly structured (us). Considering finite element discretization by P2-P1 elements Table 3.1 lists spectral condition numbers of (12). It can be seen that only the $S = h^{-1}I$ preconditioner leads to results independent of h .

The growth of the condition number in Table 3.1 due to the preconditioner with $-1/2$ power indeed confirms that $H^{1/2}$ is not appropriate in our setting. Alternatively, an attempt to establish the trace space could be based on viewing the trace as an 1/2 operator. Starting from L^2 a formal calculation then leads to the space $H^{-1/2}$ and $H^{1/2}$ as the multiplier space. While we do not include here the results for $S = (-\Delta + I)^{1/2}$ we remark that the condition number behaves practically identically to $S = I$.

In order to verify that the properties of the $h^{-1}I$ preconditioner are not due to the uniformly structured (us) mesh, we also consider refinements of two additional discretizations of Ω shown in Fig. 3, which we refer to as uniform unstructured (uu) and non-uniform unstructured (nu) respectively. In the uniform unstructured mesh, the vertices of the mesh are no longer on a uniform square grid, but the mesh elements are still close to uniform in size. In the non-uniform unstructured mesh, the vertices are not on a square grid, and the mesh elements close to Γ are finer than the ones further away.

Using these triangulations, problem (12) shall be discretized by P2-P1 elements as well P2-P0 elements to provide more evidence for the preconditioner construction. Indeed, Table 3.2 shows that the condition numbers of (12) are bounded irrespective of the underlying mesh and the finite element discretization considered.

Example 3.3 (Babuška problem with Neumann boundary conditions). Let Ω be a bounded domain with the boundary partitioned into non-overlapping subdomains $\partial\Omega = \partial\Omega_D \cup \partial\Omega_N \cup \Gamma$ such that $|\partial\Omega_D| > 0$ and $|\Gamma| > 0$. We will consider both the case that $\partial\Omega_D \cap \Gamma = \emptyset$ and later the case that $\partial\Omega_N \cap \Gamma = \emptyset$. Let $V = H_{0,\partial\Omega_D}^1(\Omega)$ and consider the problem

$$\min_{u \in V} \int_{\Omega} |\nabla u|^2 dx - 2 \int_{\Omega} fu dx \quad \text{subject to} \quad \int_{\Gamma} (\partial_{\mathbf{n}}u - g) p ds = 0. \tag{13}$$

With p the Lagrange multiplier associated with $\partial_{\mathbf{n}}$ -constraint (13) leads to a variational problem: Find $u \in V$ and $p \in Q = L^2(\Gamma)$ such that

$$\begin{aligned} \int_{\Omega} \nabla u \cdot \nabla v dx + \int_{\Gamma} p \partial_{\mathbf{n}}v ds &= \int_{\Omega} f v dx \quad \forall v \in V, \\ \int_{\Gamma} q \partial_{\mathbf{n}}u ds &= \int_{\Gamma} g q ds \quad \forall q \in Q. \end{aligned} \tag{14}$$

Table 3.3

Condition numbers of (15) discretized by P2-P1 elements on uniform refinements of (us) mesh in Fig. 3. Boundedness in discretization is obtained only with $S = h^{-1}I$.

h	$(-\Delta + I)^{1/2}$	I	$h^{-1}I$
2^{-2}	11.99	6.70	4.88
2^{-3}	14.55	9.27	4.88
2^{-4}	18.47	12.89	4.88
2^{-5}	24.44	18.01	4.88
2^{-6}	33.25	25.26	4.88
2^{-7}	45.96	35.52	4.88
2^{-8}	64.10	50.02	4.88

Table 3.4

Condition numbers of (15) using $S = h^{-1}I$ preconditioner discretized on uniform refinements of parent meshes in Fig. 3 using two element types. Refinement level is indicated by l . (Left) Γ intersects $\partial\Omega_N$. (Right) Γ intersects $\partial\Omega_D$.

l	P2-P1			P2-P0			l	P2-P1			P2-P0		
	(us)	(uu)	(nu)	(us)	(uu)	(nu)		(us)	(uu)	(nu)	(us)	(uu)	(nu)
1	4.88	4.77	6.64	3.49	3.49	3.06	1	5.34	5.25	6.67	3.48	3.45	3.04
2	4.88	5.98	6.56	3.49	3.04	3.37	2	5.34	6.25	6.67	3.49	2.99	3.37
3	4.88	5.78	5.67	3.49	3.24	3.36	3	5.34	5.94	5.84	3.49	3.24	3.36
4	4.88	6.31	6.67	3.49	3.40	3.40	4	5.34	6.52	6.93	3.49	3.40	3.40
5	4.88	5.25	5.68	3.49	3.44	3.48	5	5.34	5.56	6.07	3.49	3.44	3.48
6	4.88	5.71	5.89	3.49	3.41	3.44	6	5.34	5.91	6.17	3.49	3.41	3.44
7	4.88	6.14	6.61	3.49	3.35	3.47	7	5.34	6.40	6.85	3.49	3.35	3.47

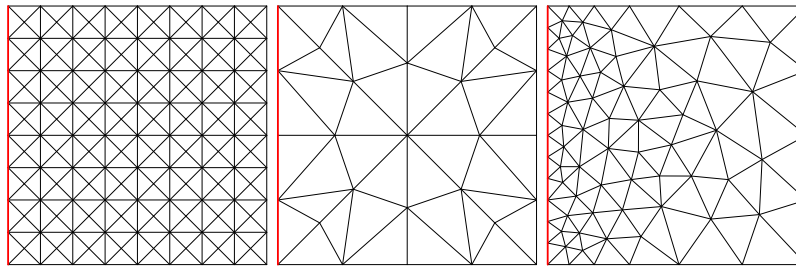


Fig. 3. Parent meshes for uniform refinement. From left to right: uniform structured (us), uniform unstructured (uu), non-uniform unstructured (nu). Non-uniform mesh has finer (by factor 3) mesh size close to Γ . (For interpretation of the references to color in this figure legend, the reader is referred to the web version of this article.)

The preconditioned continuous problem then reads

$$\mathcal{B}\mathcal{A} = \begin{pmatrix} -\Delta & \\ & S \end{pmatrix}^{-1} \begin{pmatrix} -\Delta & \partial_{\mathbf{n}}' \\ \partial_{\mathbf{n}} & \end{pmatrix}. \tag{15}$$

Following the preliminaries where $\partial_{\mathbf{n}}$ was regarded as a 3/2 operator we let $S = (-\Delta + I)^{1/2}$. Alternatively, $S = h^{-1}I$ is set following Assumption 1. Finally $S = I$ is considered. Matrix realization of the S operators shall be identical to Example 3.2. We shall also use the tessellations described in Example 3.2 as well as identical eigenvalue solvers.

To compare the three preconditioners we let Ω be a unit square and $\Gamma = \{(x, y) \in \partial\Omega, x = 0\}$ (marked in red in Fig. 3) and we consider first the (Neumann) case where $\partial\Omega_N = \{(x, y) \in \partial\Omega, y = 0 \text{ or } y = 1\}$, i.e. where the multiplier domain intersects the part of boundary with Neumann boundary conditions. On $\partial\Omega_D$, we have the Dirichlet boundary condition $u = g$, and on $\partial\Omega_N$ homogeneous Neumann condition $\nabla u \cdot \mathbf{n} = 0$ is assumed.

Using the uniform meshes (marked as (us) in Fig. 3) and P2-P1 elements, Table 3.3 shows the spectral condition numbers of (15). As in Example 3.2 only $S = h^{-1}I$ preconditioner (based on Assumption 1) leads to results independent of h .

Table 3.4 shows that the performance of $h^{-1}I$ in (15) remains robust if different tessellations and finite element discretizations are used.

In the context of multiscale problems, compatibility of boundary conditions of the multiplier space and the boundary conditions prescribed on the domain intersecting Γ is known to present an issue, cf. e.g. [12]. Here, we address this problem by considering (15) with $|\partial\Omega_N| = 0$, i.e. we let Γ intersect only the Dirichlet boundary. We remark that until this point only intersection with Neumann boundary was considered.

In Table 3.4 the Dirichlet problem is considered with an *unmodified* $h^{-1}I$ preconditioner. In particular, with P2-P1 discretization we impose *no* boundary conditions on the multiplier space. Using this construction the condition numbers can be seen to remain bounded on all the meshes and with both finite element discretizations.

We remark that the $h^{-1}I$ preconditioner is equally unaffected by the Dirichlet boundary conditions on $\partial\Omega_D = \partial\Omega \setminus \Gamma$ in the trace-constrained L^2 projection problem (10) with $V = H^1_{0,\partial\Omega_D}(\Omega)$, cf. Example 3.2. This is in contrast to the H^1 problems considered in [16], where the appropriate preconditioner was $H^{-\frac{1}{2}}$ or $H^{-\frac{1}{2}}$ depending on whether the interface intersected the Dirichlet boundary or not. Let us note that in the continuous setting boundary values have measure zero and this may then be perceived as support for our assumption that the L^2 space is the correct one in our discrete setting. Of course, the counterargument in the continuous setting is that then the trace cannot be defined. However, in the discrete setting, this can be done.

Without including the simulation results we comment here that the condition numbers of the Dirichlet problem are practically identical to those presented in Tables 3.1 and 3.2. In addition, with the two preconditioners $S = I$ and $S = (-\Delta + I)^{1/2}$ on the unstructured meshes a growth of condition numbers with h is observed similar to Table 3.3.

We remark that the stability of the preconditioner $h^{-1}I$ in Example 3.3 provides numerical evidence for well-posedness of (14), i.e. the Darcy subproblem in the coupled Darcy–Stokes system (4).

4. Robust preconditioners for the Darcy–Stokes system

In Example 2.1, we showed that the efficiency of the preconditioner (8) for the primal Darcy–Stokes problem (7) varied substantially with the material parameters even though the Stokes block and the Darcy block were preconditioned with appropriate preconditioners, and argued that the reason was a poor preconditioner at the interface. In this section we demonstrate that robustness with respect to mesh resolution and variations in material parameters can be obtained by posing the Lagrange multiplier in properly weighted fractional spaces, namely the intersection space $X_\Gamma = \sqrt{K}L^2(\Gamma) \cap \frac{1}{\sqrt{\mu}}H^{-1/2}(\Gamma)$. No modifications of the velocity or pressure space norms will be required. Our analysis is closely related to [16], and based on Assumption 1 along with an assumption of stability for the Stokes problem. We remark that although Assumption 1 is motivated by the discrete problem, our analysis is carried out in a continuous setting.

Let $\partial\Omega_i = \partial\Omega_{i,D} \cup \partial\Omega_{i,N} \cup \Gamma$ for $i = f, p$ such that $\partial\Omega_{f,D} \cap \Gamma = \emptyset$. We shall prove well-posedness of the coupled Darcy–Stokes problem (4) with spaces

$$V_f = \sqrt{\mu}H^1_{0,D}(\Omega_f) \cap \sqrt{D}L^2_\tau(\Gamma), Q_f = \frac{1}{\sqrt{\mu}}L^2(\Omega_f), Q_p = \sqrt{K}H^1_{0,D}(\Omega_p), X_\Gamma = \sqrt{K}L^2(\Gamma) \cap \frac{1}{\sqrt{\mu}}H^{-1/2}(\Gamma). \tag{16}$$

Note that in case Γ intersects only the Dirichlet boundary $\partial\Omega_{f,D}$ the space $H^{-1/2}$ needs to be modified to reflect $H^{1/2}_{00}$ as the appropriate trace space of V_f . We refer to [16] for a thorough discussion of the subject.

As a prerequisite for the coupled problem to be well-posed, we require that each subproblem is well-posed. For the Stokes subproblem the property has been demonstrated by numerical experiments in [16]. Here we state the result without proof.

Assumption 2. Let Ω_f be such that $\partial\Omega_f = \partial\Omega_{f,D} \cup \partial\Omega_{f,N} \cup \Gamma$, $|\partial\Omega_{f,D}| > 0$ and $\partial\Omega_{f,D} \cap \Gamma = \emptyset$. We define $V_S = \sqrt{\mu}H^1_{0,D}(\Omega_f) \cap \sqrt{D}L^2_\tau(\Gamma) \times \frac{1}{\sqrt{\mu}}L^2(\Omega_f) \times \frac{1}{\sqrt{\mu}}H^{-1/2}(\Gamma)$ and the forms

$$a_S((\mathbf{u}_f, p_f, \lambda), (\mathbf{v}_f, q_f, w)) = \mu(\nabla \mathbf{u}_f, \nabla \mathbf{v}_f) + D(\mathbf{u}_f \cdot \boldsymbol{\tau}, \mathbf{v}_f \cdot \boldsymbol{\tau})_\Gamma + (p_f, \nabla \cdot \mathbf{v}_f) + (\nabla \cdot \mathbf{u}_f, q_f) + (T_n \mathbf{u}_f, w)_\Gamma + (\lambda, T_n \mathbf{v}_f)_\Gamma, \\ L_S((\mathbf{v}_f, q_f, w)) = (\mathbf{f}, \mathbf{v}_f) + (g, q_f) + (h_D, w)_\Gamma,$$

where $\mathbf{f} \in \frac{1}{\sqrt{\mu}}H^{-1}(\Omega_f)$, $g \in \sqrt{\mu}L^2(\Omega_f)$, $h_D \in \sqrt{\mu}H^{\frac{1}{2}}(\Gamma)$ are arbitrary. Then we assume that the Stokes problem: Find $(\mathbf{u}_f, q_f, \lambda) \in V_S$ such that

$$a_S((\mathbf{u}_f, p_f, \lambda), (\mathbf{v}_f, q_f, w)) = L_S((\mathbf{v}_f, q_f, w)) \quad \forall (\mathbf{v}_f, q_f, w) \in V_S$$

satisfies the Brezzi conditions and hence has a unique solution $(\mathbf{u}_f, p_f, \lambda) \in V_S$ and the following bound holds

$$\|(\mathbf{u}_f, p_f, \lambda)\|_{V_S} \leq C \left(\|\mathbf{f}\|_{\frac{1}{\sqrt{\mu}}H^{-1}(\Omega_f)}^2 + \|g\|_{\sqrt{\mu}L^2(\Omega_f)}^2 + \|h_D\|_{\sqrt{\mu}H^{\frac{1}{2}}(\Gamma)}^2 \right)^{\frac{1}{2}}.$$

Here the constant C depends only on Ω_f , $\partial\Omega_{f,D}$ and Γ .

Corresponding well-posedness of the Darcy problem with ∂_n -constraint was demonstrated numerically for $K = 1$ in Example 3.3. Here, we analyze the general case.

Lemma 1. Suppose Ω_p, Γ are such that Assumption 1 holds and $|\partial\Omega_{p,D}| > 0$. Then for any $f \in \frac{1}{\sqrt{K}}H^{-1}(\Omega_p)$, $h \in \frac{1}{\sqrt{K}}L^2(\Gamma)$, the problem of finding $(p_p, \lambda) \in \sqrt{K}H^1_{0,D}(\Omega_p) \times \sqrt{K}L^2(\Gamma)$ so that

$$K(\nabla p_p, \nabla q_p)_{\Omega_p} + K(\lambda, \partial_n \epsilon q_p)_\Gamma = (f, q_p) \quad \forall q_p \in \sqrt{K}H^1_{0,D}(\Omega_p), \\ K(\partial_n \epsilon p_p, w)_\Gamma = (h, w)_\Gamma \quad \forall w \in \sqrt{K}L^2(\Gamma) \tag{17}$$

has a unique solution satisfying

$$\|p_p\|_{\sqrt{K}H_{0,D}^1(\Omega_p)} \leq C \left(\|h\|_{\frac{1}{\sqrt{K}}L^2(\Gamma)}^2 + \|f\|_{\frac{1}{\sqrt{K}}H^{-1}(\Omega_p)}^2 \right)^{\frac{1}{2}},$$

where C is a constant depending only on Ω_p .

Proof. Let $V = \sqrt{K}H_{0,D}^1(\Omega_p)$, $Q = \sqrt{K}L^2(\Gamma)$. We consider the left-hand side of (3) as an operator

$$\begin{pmatrix} A & B' \\ B & \end{pmatrix} : V \times Q \rightarrow V' \times Q', \tag{18}$$

where $(Ap_p, q_p) = K(\nabla p_p, \nabla q_p)_{\Omega_p}$ and $(Bp_p, w) = K(\partial_{\mathbf{n},\epsilon} p_p, w)_{\Gamma}$.

The statement of the theorem follows from the Brezzi theory [35] once the Brezzi conditions are verified. That is, we must show that A, B are bounded, A is coercive on $\ker B$ and that the inf-sup condition $\inf_{q \in Q} \sup_{v \in V} (Bv, q) \geq \beta \|v\| \|q\|$ holds for some constant $\beta > 0$.

Here the boundedness of A and the coercivity on V are evident. For the latter we recall that $|\partial\Omega_{p,D}| > 0$ is assumed and invoke the Poincare inequality. Assumption 1 is needed to show the properties of B . Because

$$K(\lambda, \partial_{\mathbf{n},\epsilon} q_p)_{\Gamma} \leq K \|\lambda\|_{\sqrt{K}L^2(\Gamma)} \|\partial_{\mathbf{n},\epsilon} q_p\|_{\frac{1}{\sqrt{K}}L^2(\Gamma)} \leq \|\partial_{\mathbf{n},\epsilon}\| \|\lambda\|_{\sqrt{K}L^2(\Gamma)} \|q_p\|_{\sqrt{K}H^1(\Omega_p)},$$

we have boundedness with constant $\|\partial_{\mathbf{n},\epsilon}\|$. For the inf-sup condition, we recall the bounded right inverse E of $\partial_{\mathbf{n},\epsilon}$. Letting $p_p^* = E(\lambda)$, we have $K(\lambda, \partial_{\mathbf{n},\epsilon} p_p^*) = \|\lambda\|_{\sqrt{K}L^2(\Gamma)}^2$ and $\|p_p^*\|_{\sqrt{K}H_{0,D}^1(\Omega_p)} \leq \|E\| \|\lambda\|_{\sqrt{K}L^2(\Gamma)}$ so that

$$\sup_{p_p \in \sqrt{K}H_{0,D}^1(\Omega_p)} \frac{K(\lambda, \partial_{\mathbf{n},\epsilon} p_p)}{\|p_p\|_{\sqrt{K}H_{0,D}^1(\Omega_p)}} \geq \frac{K(\lambda, \partial_{\mathbf{n},\epsilon} p_p^*)}{\|p_p^*\|_{\sqrt{K}H_{0,D}^1(\Omega_p)}} = \frac{\|\lambda\|_{\sqrt{K}L^2(\Gamma)}^2}{\|p_p^*\|_{\sqrt{K}H_{0,D}^1(\Omega_p)}} \geq \frac{\|\lambda\|_{\sqrt{K}L^2(\Gamma)}^2}{\|E\| \|\lambda\|_{\sqrt{K}L^2(\Gamma)}} \geq \frac{1}{\|E\|} \|\lambda\|_{\sqrt{K}L^2(\Gamma)}.$$

This proves all the Brezzi conditions. \square

Having discussed well-posedness of the Stokes and Darcy subproblems our main result concerning the coupled Darcy–Stokes problem (4) is given in Theorem 1. We remark that given two well-posed subproblems the coupled system could be analyzed with the framework of [16]. Here we provide a standalone proof.

Theorem 1. Let Ω_f, Ω_p be as defined in Assumption 1 and Assumption 2. Further let

$$V_f = \sqrt{\mu}H_{0,D}^1(\Omega_f) \cap \sqrt{D}L^2_{\tau}(\Gamma), Q_f = \frac{1}{\sqrt{\mu}}L^2(\Omega_f), Q_p = \sqrt{K}H_{0,D}^1(\Omega_p), X_{\Gamma} = \sqrt{K}L^2(\Gamma) \cap \frac{1}{\sqrt{\mu}}H^{-1/2}(\Gamma).$$

Then the operator \mathcal{A} in (7) is an isomorphism mapping W to its dual space W' such that $\|\mathcal{A}\|_{\mathcal{L}(W,W')} \leq C$ and $\|\mathcal{A}^{-1}\|_{\mathcal{L}(W',W)} \leq \frac{1}{c}$, where C is independent of μ, K , and D .

Proof of Theorem 1. We aim to apply Brezzi theory [35] to the Darcy–Stokes operator (7) in the abstract form (18). To this end let $V = V_f \times Q_p$ and $Q = Q_f \times X_{\Gamma}$ where for brevity $X_f = \frac{1}{\sqrt{\mu}}H^{-1/2}(\Gamma)$, $X_p = \sqrt{K}L^2(\Gamma)$ and we let the operators A, B be defined in terms of bilinear forms from (5) as

$$\begin{aligned} (A(\mathbf{u}_f, p_p), (\mathbf{v}_f, q_p)) &= \mu(\nabla \mathbf{u}_f, \nabla \mathbf{v}_f)_{\Omega_f} + D(\mathbf{u}_f \cdot \boldsymbol{\tau}, \mathbf{v}_f \cdot \boldsymbol{\tau})_{\Gamma} + K(\nabla p_p, \nabla q_p)_{\Omega_p}, \\ (B(\mathbf{u}_f, p_p), (q_f, w)) &= (\nabla \cdot \mathbf{u}_f, q_f)_{\Gamma} + (T_{\mathbf{n}} \mathbf{u}_f, w)_{\Gamma} - K(\partial_{\mathbf{n},\epsilon} p_p, w)_{\Gamma}. \end{aligned}$$

We proceed to verify the Brezzi conditions. Note that by assumption $|\partial\Omega_{i,D}| > 0$, $i = p, f$ so that by Poincare inequality on both subdomains A is coercive. For boundedness of A observe that $\mu(\nabla \mathbf{u}_f, \nabla \mathbf{v}_f) + D(\mathbf{u}_f \cdot \boldsymbol{\tau}, \mathbf{v}_f \cdot \boldsymbol{\tau})_{\Gamma} \leq \|\mathbf{u}_f\|_{V_f} \|\mathbf{v}_f\|_{V_f}$ by Cauchy–Schwarz inequality. Moreover, following Lemma 1, we have $K(\nabla p_p, \nabla q_p) \leq \|p_p\|_{Q_p} \|q_p\|_{Q_p}$. Combining the two bounds and applying the Cauchy–Schwarz inequality,

$$(A(\mathbf{u}_f, p_p), (\mathbf{v}_f, q_p)) \leq \|\mathbf{u}_f\|_{V_f} \|\mathbf{v}_f\|_{V_f} + \|p_p\|_{Q_p} \|q_p\|_{Q_p} \leq \|(\mathbf{u}_f, p_p)\|_V \|(\mathbf{v}_f, q_p)\|_V.$$

To show boundedness of B we recall that $\|\nabla \cdot \mathbf{u}_f\|_{Q_f} = \|\nabla \cdot \mathbf{u}_f\|_{\sqrt{\mu}L^2(\Omega_f)} \leq C \|\mathbf{u}_f\|_{V_f}$, where C depends on the dimensionality of Ω_f . Further, by the trace inequality $\|T_{\mathbf{n}} \mathbf{u}_f\|_{X_f} = \|T_{\mathbf{n}} \mathbf{u}_f\|_{\frac{1}{\sqrt{\mu}}H^{-1/2}(\Gamma)} \leq \|T_{\mathbf{n}}\| \|\mathbf{u}_f\|_{V_f}$, and by Assumption 1 $\|K \partial_{\mathbf{n},\epsilon} p_p\|_{X_p} = \|K \partial_{\mathbf{n},\epsilon} p_p\|_{\frac{1}{\sqrt{K}}L^2(\Gamma)} = \|\partial_{\mathbf{n},\epsilon} p_p\|_{\sqrt{K}L^2(\Gamma)} \leq \|\partial_{\mathbf{n},\epsilon}\| \|p_p\|_{Q_p}$. Hence, per definition of dual norms,

$$(\nabla \cdot \mathbf{u}_f, q_f)_{\Gamma} + (T_{\mathbf{n}} \mathbf{u}_f, w)_{\Gamma} \leq \|\nabla \cdot \mathbf{u}_f\|_{Q_f} \|q_f\|_{Q_f} + \|T_{\mathbf{n}} \mathbf{u}_f\|_{X_f} \|w\|_{X_f} \leq \max(1, C) \|\mathbf{u}_f\|_{V_f} (\|q_f\|_{Q_f} + \|w\|_{X_f})$$

and

$$K(\partial_{\mathbf{n},\epsilon} p_p, w)_{\Gamma} \leq \|K \partial_{\mathbf{n},\epsilon} p_p\|_{X_p} \|w\|_{X_p} \leq \|\partial_{\mathbf{n},\epsilon}\| \|p_p\|_{Q_p} \|w\|_{X_p}.$$

Combining the two estimates we show boundedness of B

$$(B(\mathbf{u}_f, p_p), (q_f, w)) \leq 2 \max(1, C, \|T_n\|, \|\partial_{n,\epsilon}\|) \|(\mathbf{u}_f, p_p)\|_V \| (q_f, w) \|_Q.$$

Finally, we turn to the inf-sup condition. Let $R_{Q_f}^{-1}, R_{X_f}^{-1}, R_{X_p}^{-1}$ be the inverse Riesz maps of their respective spaces, so that $R_V u = (u, \cdot)_V \in V'$. Let $(q_f, w) \in Q_f \times X$ be arbitrary. We first define two extensions by using the two subproblems. Recalling the notation of Assumption 2, let $(\mathbf{u}_f^*, p_f^*, \lambda_1^*)$ be the solution of

$$a_S((\mathbf{u}_f^*, p_f^*, \lambda_1^*), (\mathbf{v}_f, q_f', w')) = (R_{Q_f}^{-1} q_f, q_f') + (R_{X_f}^{-1} w, w')_T \text{ for all } (\mathbf{v}_f, q_f', w') \in V_S.$$

Per assumption, there is a constant C_f so that we have the bound

$$\|\mathbf{u}_f^*\|_{V_f} \leq C_f \left(\|R_{Q_f}^{-1} q_f\|_{\sqrt{\mu}L^2(\Omega_f)}^2 + \|R_{X_f}^{-1} w\|_{\sqrt{\mu}H^{\frac{1}{2}}(\Gamma)}^2 \right)^{\frac{1}{2}} = C_f \left(\|q_f\|_{Q_f}^2 + \|w\|_{X_f}^2 \right)^{\frac{1}{2}}, \tag{19}$$

where the right equality follows from the fact that $\sqrt{\mu}L^2(\Omega_f) = Q_f'$, $\sqrt{\mu}H^{\frac{1}{2}}(\Gamma) = X_f'$ and that the Riesz map is an isometry. Similarly, let p_p^*, λ_2^* be the solution of

$$K(\nabla p_p^*, \nabla q_p')_{\Omega_p} + K(\lambda_2^*, \partial_{n,\epsilon} q_p')_T + K(\partial_{n,\epsilon} p_p^*, w')_T = (R_{X_p}^{-1} w, w')_T \quad (q_p', w') \in \sqrt{K}H_{0,D}^1(\Omega_p) \times \sqrt{K}L^2(\Gamma).$$

By Lemma 1, we then have the bound

$$\|p_p^*\|_{Q_p} \leq C_p \|R_{X_p}^{-1} w\|_{\frac{1}{\sqrt{K}}L^2(\Gamma)} = C_p \|w\|_{X_p} \tag{20}$$

for a constant C_p . Observe now that by our definitions of \mathbf{u}_f^*, p_p^* ,

$$\begin{aligned} (\nabla \cdot \mathbf{u}_f^*, q_f)_T + (T_n \mathbf{u}_f^*, w)_T - K(\partial_{n,\epsilon} p_p^*, w)_T &= (R_{Q_f}^{-1} q_f, q_f)_T + (R_{X_f}^{-1} w, w)_T - (R_{X_p}^{-1} w, w)_T \\ &= \|q_f\|_{Q_f}^2 + \|w\|_{X_f}^2 + \|w\|_{X_p}^2 = \|q_f\|^2 + \|w\|_X^2. \end{aligned}$$

Using (19), (20)

$$\|(\mathbf{u}_f^*, p_p^*)\|_V = \left(\|\mathbf{u}_f^*\|_{V_f}^2 + \|p_p^*\|_{Q_p}^2 \right)^{\frac{1}{2}} \leq C \left(\|q_f\|_{Q_f}^2 + \|w\|_{X_f}^2 + \|w\|_{X_p}^2 \right)^{\frac{1}{2}} = C \left(\|q_f\|_{Q_f}^2 + \|w\|_X^2 \right)^{\frac{1}{2}},$$

where $C = \max(C_f, C_p)$. Putting this together, we can prove the inf-sup condition:

$$\begin{aligned} \sup_{(\mathbf{u}_f, p_p) \in V} \frac{(\nabla \cdot \mathbf{u}_f, q_f)_T + (T_n \mathbf{u}_f, w)_T - K(\partial_{n,\epsilon} p_p, w)_T}{\|(\mathbf{u}_f, p_p)\|_V} &\geq \frac{(\nabla \cdot \mathbf{u}_f^*, q_f)_T + (T_n \mathbf{u}_f^*, w)_T - K(\partial_{n,\epsilon} p_p^*, w)_T}{\|(\mathbf{u}_f^*, p_p^*)\|_V} \\ &\geq \frac{1}{C} \frac{\|q_f\|^2 + \|w\|_X^2}{\left(\|q_f\|_{Q_f}^2 + \|w\|_X^2 \right)^{\frac{1}{2}}} = \frac{1}{C} \|(q_f, w)\|_Q. \end{aligned}$$

Hence, the inf-sup condition holds with $\beta = \frac{1}{C}$. By Brezzi theory, Theorem 1 follows, and the problem is well-posed. As in the argument of [16], we note that due to our use of parameter weighted spaces, all constants are in fact independent of the problem parameters, and the operator preconditioner is therefore robust to parameter variations. \square

Using operator preconditioning and Theorem 1 a suitable preconditioner for the primal Darcy–Stokes problem (4) is a Riesz map with respect to the inner product of W in (16), that is, the operator

$$\mathcal{B} = \left(\begin{array}{cc} -\mu \Delta + DT'_\tau T_\tau & \\ & K \Delta \\ \hline & \frac{1}{\mu} I \\ & -\mu (I + \Delta)^{-1/2} + \frac{\kappa}{h} I \end{array} \right)^{-1}. \tag{21}$$

We remark that all of the components of the preconditioner can be realized in an efficient, order optimal manner with multilevel schemes. In particular, the only non-standard component here is the multilevel scheme for the fractional operator which, however, has been established in [18].

Example 4.1 (Robust Darcy–Stokes preconditioning). We consider the setup from Example 2.1, i.e., a P2–P1–P2–P0 discretization, while using the operator (21) as preconditioner. As before, the leading blocks of the preconditioner are realized using single algebraic multigrid V-cycle. The multiplier block is then assembled using the eigenvalue decomposition and its inverse is computed by a direct solver.

The obtained iteration and condition numbers are plotted in Fig. 4. It can be seen that both quantities are bounded in mesh size N as well as the physical parameters μ, κ and α_{BJS} .

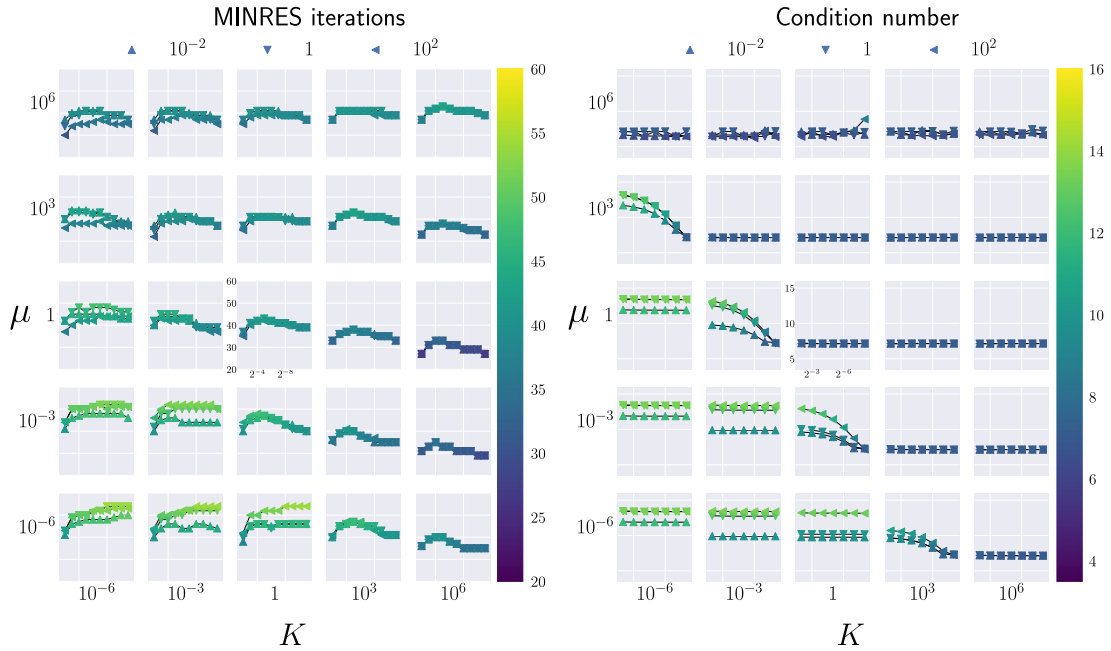


Fig. 4. Mesh refinement vs. iteration counts (left) and condition numbers (right) for **Example 4.1** using the preconditioner (21). All subplots share x - and y -axes. For fixed μ , K the x -axis range in the iterations subplot extends from $h = 2^{-2}$ to $h = 2^{-11}$. In conditioning plots the range is from $h = 2^{-2}$ to $h = 2^{-8}$. The value of α_{BJS} is indicated by the line marker. Triangular markers on top of each other look like squares.

Example 4.2 (Alternative choices of function spaces for the coupled problem). As demonstrated in **Example 3.3**, the Darcy subproblem also appears to be stable when discretized by P2-P1 elements. According to the reasoning given in [16], we would therefore expect our preconditioner for the coupled problem to remain robust if we instead use a P1 element for the multiplier. Additionally, because the P2-P0 element is known to be stable for the Stokes problem, we would also expect that our preconditioner would remain robust if the P2-P0 element was used to discretize the Stokes subproblem instead.

Altogether, this suggests three new discretizations for the coupled problem: $V_f \times Q_f \times Q_p \times X = \text{P2-P0-P2-P0}$, P2-P0-P2-P1 , or P2-P1-P2-P1 . We repeat the experiment performed in **Example 4.1** for all three discretizations. The results for $\alpha_{\text{BJS}} = 1$ are shown in **Fig. 5**. It can be seen that the preconditioner appears robust both in the mesh size and in the physical parameters for all three choices of discretizations. We remark that experiments were also carried out with $\alpha_{\text{BJS}} = 10^{-2}$ and 10^2 . The results were substantially similar to **Example 4.1**, and for legibility are therefore not shown.

Remark 1. Below we consider the validity of **Assumption 1** in a continuous and discrete setting. Clearly, in a continuous setting it is easy to find a function that violates the assumption. Consider the case where $\epsilon \ll h$ while Ω and Γ are both unit sized. Further, let $u \in H^1(\Omega_p)$ be a function which is zero in $\Omega \setminus \Gamma_\epsilon$ and has a gradient of 1 in Γ_ϵ . Recalling our definition of the operator $\partial_{\mathbf{n},\epsilon} : H^1(\Omega_p) \rightarrow L^2(\Gamma_\epsilon)$ by

$$\int_{\Gamma} \partial_{\mathbf{n},\epsilon} u \cdot w \, ds = \frac{1}{\epsilon} \int_{\Gamma_\epsilon} \nabla u \cdot \mathbf{n}_{\Gamma_\epsilon} E_\epsilon w \, dx,$$

we see that $\partial_{\mathbf{n},\epsilon} u \in L^2(\Gamma_\epsilon)$ is the unit constant function whereas $\|u\|_1 \approx \sqrt{\epsilon}$. Hence $\|\partial_{\mathbf{n},\epsilon}\| \geq \frac{\|\partial_{\mathbf{n},\epsilon} u\|_{L^2(\Gamma_\epsilon)}}{\|u\|_{H^1(\Omega_p)}} \approx \frac{1}{\sqrt{\epsilon}}$, which is very large for small ϵ . Clearly, this function violates **Assumption 1**.

The above construction of a function that violates the assumption is however clearly not relevant in our discrete setting as these functions are below the resolution of our finite element mesh. Indeed, in our numerical experiments, we use discrete subspaces of $H^1(\Omega_p)$, so that any function whose gradient is nonzero on Γ also has nonzero gradient at distance h from Γ . This means that if ϵ is chosen smaller than h , functions like u above which are zero immediately outside of Γ_ϵ are not admissible.

For a relevant finite element function u_h , constructed as above, i.e., such that u_h is zero everywhere except having a gradient of 1 on the finite elements with facets on Γ , assuming that $\epsilon \ll h$, we have $\frac{\|\partial_{\mathbf{n},\epsilon} u_h\|_{L^2(\Gamma_\epsilon)}}{\|u_h\|_{H^1(\Omega_p)}} \approx \frac{1}{\sqrt{h}}$. Indeed this estimate corresponds to the scaling shown in **Examples 3.2** and **3.3**.

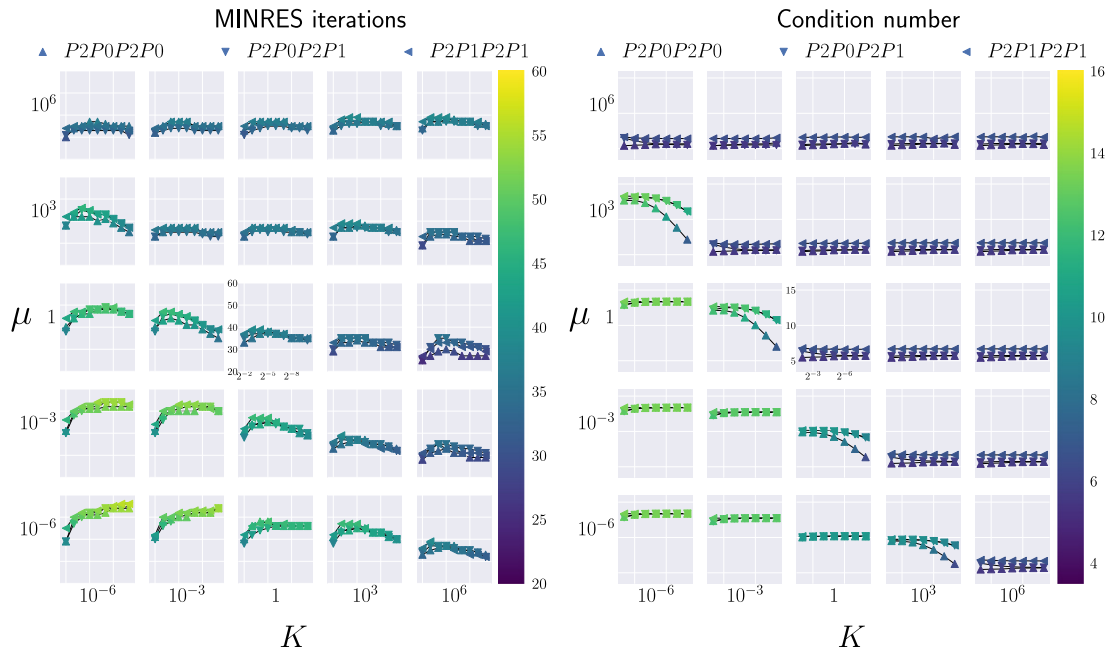


Fig. 5. Mesh refinement vs. iteration counts (left) and condition numbers (right) for alternative discretizations. The line marker indicates the discretization used. All subplots share x - and y -axes and have $\alpha_{\text{BJS}} = 1$. For fixed μ , K the x -axis range in the iterations subplot extends from $h = 2^{-2}$ to $h = 2^{-10}$. In conditioning plots the range is from $h = 2^{-2}$ to $h = 2^{-8}$.

Acknowledgments

Karl Erik Holter is a doctoral fellow in the Simula-UCSD-University of Oslo Research and PhD training (SUURPh) program, an international collaboration in computational biology and medicine funded by the Norwegian Ministry of Education and Research. Miroslav Kuchta acknowledges support by the Research Council of Norway (NFR) grant 280709. Kent-Andre Mardal acknowledges support by the Research Council of Norway (NFR) grants 280709 and 301013.

References

- [1] T. Arbogast, D.S. Brunson, A computational method for approximating a Darcy–Stokes system governing a vuggy porous medium, *Comput. Geosci.* 11 (3) (2007) 207–218.
- [2] G. Johnny, N. Michael, A family of nonconforming elements for the Brinkman problem, *IMA J. Numer. Anal.* 32 (4) (2012) 1484–1508.
- [3] T. Karper, K.-A. Mardal, R. Winther, Unified finite element discretizations of coupled Darcy–Stokes flow, *Numer. Methods Partial Differential Equations* 25 (2) (2009) 311–326.
- [4] K.A. Mardal, X.-C. Tai, R. Winther, A robust finite element method for Darcy–Stokes flow, *SIAM J. Numer. Anal.* 40 (5) (2002) 1605–1631.
- [5] S. Zhang, X. Xie, Y. Chen, Low order nonconforming rectangular finite element methods for Darcy–Stokes problems, *J. Comput. Math.* (2009) 400–424.
- [6] E. Burman, P. Hansbo, A unified stabilized method for Stokes’ and Darcy’s equations, *J. Comput. Appl. Math.* 198 (1) (2007) 35–51.
- [7] M.-F. Feng, R.-S. Qi, R. Zhu, B.-t. Ju, Stabilized Crouzeix–Raviart element for the coupled Stokes and Darcy problem, *App. Math. Mech* 31 (3) (2010) 393–404.
- [8] Q. Hong, J. Kraus, J. Xu, L. Zikatanov, A robust multigrid method for discontinuous Galerkin discretizations of Stokes and linear elasticity equations, *Numer. Math.* 132 (1) (2016) 23–49.
- [9] Q. Hong, J. Kraus, Uniformly stable discontinuous Galerkin discretization and robust iterative solution methods for the Brinkman problem, *SIAM J. Numer. Anal.* 54 (5) (2016) 2750–2774.
- [10] X. Xie, J. Xu, G. Xue, Uniformly-stable finite element methods for Darcy–Stokes–Brinkman models, *J. Comput. Math.* (2008) 437–455.
- [11] W.J. Layton, F. Schieweck, I. Yotov, Coupling fluid flow with porous media flow, *SIAM J. Numer. Anal.* 40 (6) (2002) 2195–2218.
- [12] J. Galvis, M. Sarkis, Non-matching mortar discretization analysis for the coupling Stokes–Darcy equations, *Electron. Trans. Numer. Anal.* 26 (2007) 07.
- [13] B. Rivière, I. Yotov, Locally conservative coupling of Stokes and Darcy flows, *SIAM J. Numer. Anal.* 42 (5) (2005) 1959–1977.
- [14] G.N. Gatica, S. Meddahi, R. Oyarzúa, A conforming mixed finite-element method for the coupling of fluid flow with porous media flow, *IMA J. Numer. Anal.* 29 (1) (2008) 86–108.
- [15] M. Discacciati, A. Quarteroni, Navier–Stokes/Darcy coupling: modeling, analysis, and numerical approximation, 2009.
- [16] K.E. Holter, M. Kuchta, K.-A. Mardal, Robust preconditioning of monolithically coupled multiphysics problems, 2020, arXiv preprint arXiv: 2001.05527.
- [17] J. Bramble, J. Pasciak, P. Vassilevski, Computational scales of Sobolev norms with application to preconditioning, *Math. Comp.* 69 (230) (2000) 463–480.
- [18] T. Bærland, M. Kuchta, K.-A. Mardal, Multigrid methods for discrete fractional Sobolev spaces, *SIAM J. Sci. Comput.* 41 (2) (2019) A948–A972.

- [19] M. Discacciati, A. Quarteroni, Analysis of a domain decomposition method for the coupling of Stokes and Darcy equations, in: *Numerical Mathematics and Advanced Applications*, Springer, 2003, pp. 3–20.
- [20] M. Cai, M. Mu, J. Xu, Preconditioning techniques for a mixed Stokes/Darcy model in porous media applications, *J. Comput. Appl. Math.* 233 (2) (2009) 346–355.
- [21] M. Discacciati, A. Quarteroni, A. Valli, Robin–Robin domain decomposition methods for the Stokes–Darcy coupling, *SIAM J. Numer. Anal.* 45 (3) (2007) 1246–1268.
- [22] Z. Ding, A proof of the trace theorem of Sobolev spaces on Lipschitz domains, *Proc. Amer. Math. Soc.* 124 (2) (1996) 591–600.
- [23] M. Kuchta, M. Nordaas, J.C. Verschaeve, M. Mortensen, K.-A. Mardal, Preconditioners for saddle point systems with trace constraints coupling 2d and 1d domains, *SIAM J. Sci. Comput.* 38 (6) (2016) B962–B987.
- [24] T.J. Hughes, J.A. Cottrell, Y. Bazilevs, Isogeometric analysis: CAD, finite elements, NURBS, exact geometry and mesh refinement, *Comput. Methods Appl. Mech. Engrg.* 194 (39–41) (2005) 4135–4195.
- [25] T. Nilssen, X.-C. Tai, R. Winther, A robust nonconforming H^2 -element, *Math. Comp.* 70 (234) (2001) 489–505.
- [26] A. Mikelić, W. Jäger, On the interface boundary condition of Beavers, Joseph, and Saffman, *SIAM J. Appl. Math.* 60 (4) (2000) 1111–1127.
- [27] K.-A. Mardal, R. Winther, Preconditioning discretizations of systems of partial differential equations, *Numer. Linear Algebra Appl.* 18 (1) (2011) 1–40.
- [28] A. Logg, K. Mardal, G. Wells, Automated solution of differential equations by the finite element method: The FEniCS book, in: *Lecture Notes in Computational Science and Engineering*, Springer, Berlin, Heidelberg, 2012.
- [29] M. Kuchta, Assembly of multiscale linear PDE operators, 2019, arXiv preprint [arXiv:1912.09319](https://arxiv.org/abs/1912.09319).
- [30] R.D. Falgout, U.M. Yang, Hypre: A library of high performance preconditioners, in: *International Conference on Computational Science*, Springer, 2002, pp. 632–641.
- [31] S. Balay, S. Abhyankar, M.F. Adams, J. Brown, P. Brune, K. Buschelman, L. Dalcin, A. Dener, V. Eijkhout, W.D. Gropp, D. Karpeyev, D. Kaushik, M.G. Knepley, D.A. May, L.C. McInnes, R.T. Mills, T. Munson, K. Rupp, P. Sanan, B.F. Smith, S. Zampini, H. Zhang, H. Zhang, PETSc Web page, 2019, URL <https://www.mcs.anl.gov/petsc>.
- [32] V. Hernandez, J.E. Roman, V. Vidal, SLEPC: A scalable and flexible toolkit for the solution of eigenvalue problems, *ACM Trans. Math. Software* 31 (3) (2005) 351–362.
- [33] K.E. Holter, M. Kuchta, K.-A. Mardal, Sub-voxel perfusion modeling in terms of coupled 3d-1d problem, in: *European Conference on Numerical Mathematics and Advanced Applications*, Springer, 2017, pp. 35–47.
- [34] I. Babuška, The finite element method with Lagrangian multipliers, *Numer. Math.* 20 (3) (1973) 179–192.
- [35] F. Brezzi, On the existence, uniqueness and approximation of saddle-point problems arising from Lagrangian multipliers, *Publications mathématiques et informatique de Rennes S4* (1974) 1–26.